Teagle, D.A.H., Wilson, D.S., Acton, G.D., and Vanko, D.A. (Eds.)
Proceedings of the Ocean Drilling Program, Scientific Results Volume 206

3. Analytical Sediment Chemistry on Board the *JOIDES Resolution*: A Comparison of Shipboard and Shore-Based Sample Preparation Protocols[1]

C.L. Ziegler[2] and R.W. Murray[2]

ABSTRACT

We measured the chemical composition of 100 samples from the 250-m sediment sequence retrieved from Ocean Drilling Program Site 1256 in the Guatemala Basin using a newly developed microwave-assisted acid digestion protocol followed by inductively coupled plasma–atomic emission spectroscopy (ICP-AES) analysis. We compared these data gathered onshore to the results from the flux fusion prepared samples analyzed by shipboard ICP-AES during the leg and published in the Leg 206 *Initial Reports* volume, as well as to 35 randomly selected samples that were prepared by flux fusion at Boston University and analyzed by ICP-AES. Comparison of the newly developed acid digestion protocol to shore-based flux fusion demonstrates that the microwave-assisted acid technique yields a complete digestion, and because this procedure includes boric acid, it is safe for use with HF acid as boric acid neutralizes excess HF. The precision for nearly all elements in shore-based acid digestions is better than 3% of the measured values, including for elements such as Ni, Cr, and V, which are typically difficult to measure in biogenic-rich sediments. The shore-based flux fusions, while better than shipboard reported precision values (as expected), has precision better than 3% of their respective measured values for all major elements (Si, Al, Ti, Fe, Mn, Ca, Mg, Na, and K) and several trace elements (Ba and Sr). Results for P, Cr, Ni, V, Sc, and Zr are better than 5% of their measured values. Not only does the newly developed acid digestion provide better analytical results than the typical flux fusion method,

[1] Ziegler, C.L., and Murray, R.W., 2007. Analytical sediment chemistry on board the *JOIDES Resolution*: a comparison of shipboard and shore-based sample preparation protocols. *In* Teagle, D.A.H., Wilson, D.S., Acton, G.D., and Vanko, D.A. (Eds.), *Proc. ODP, Sci. Results,* 206: College Station, TX (Ocean Drilling Program), 1–26. doi:10.2973/odp.proc.sr.206.009.2007
[2] Department of Earth Sciences, Boston University, Boston MA 02215, USA. Correspondence author: **rickm@bu.edu**

Initial receipt: 3 May 2005
Acceptance: 20 September 2005
Web publication: 1 February 2007
Ms 206SR-009

the shore-based acid procedure also exhibits downhole lithologic and chemical characteristics similar to the shipboard flux fusion prepared results. These results confirm that the current shipboard methods are adequate for first-order geochemical interpretations and that the microwave-assisted acid digestion holds great potential to be the primary technique of preparing sediments on future Integrated Ocean Drilling Program expeditions.

INTRODUCTION

With the addition of inductively coupled plasma–atomic emission spectroscopy (ICP-AES) to the chemical laboratories on the *JOIDES Resolution* (Murray et al., 2000), shipboard scientists have been able to generate extensive, near real time elemental databases on expeditions targeting paleoceanographic (e.g., Leg 199: Lyle, Wilson, Janecek, et al., 2002), geochemical (e.g., Leg 204: Tréhu, Bohrmann, Rack, Torres, et al., 2003), and igneous (e.g., Leg 187: Christie, Pedersen, Miller, et al., 2001) objectives. Sediment chemists in particular have been able to quickly and accurately characterize stratigraphic sequences, calculate mass accumulation rates of different sediment components, and provide first-order paleoceanographic interpretations throughout the duration of a cruise. Now, with the potential for a significant retooling of the shipboard preparation and analytical capabilities, possibly including ICP–mass spectrometry (ICP-MS), the preparation of samples for which is essentially identical to that for ICP-AES, with the onset of the Integrated Ocean Drilling Program (IODP), shipboard scientists will have the capability of extending the element menu to less abundant trace elements and broadening initial geochemical interpretations. Therefore, in order to further quantify the effectiveness of the Ocean Drilling Program (ODP) sample preparation protocol for future IODP expeditions in which ICP-AES or ICP-MS will be used, we compared shipboard ICP-AES initial results generated during Leg 206 to shore-based results generated by ICP-AES and ICP-MS using the Analytical Geochemistry Facility in the Department of Earth Sciences at Boston University.

ICP SAMPLE PREPARATION

Analysis by ICP spectroscopy (with the exception of laser ablation systems), requires samples to be completely dissolved (digested) into a solution. Sediment digestions are most commonly achieved either by lithium metaborate ($LiBO_2$) flux fusion or by a combined acid attack, using one or more of hydroflouric (HF), nitric (HNO_3), and hydrochloric (HCl) acids. Current shipboard procedures for the ICP-AES, following Murray et al. (2000) and Quintin et al. (2002), recommend using flux fusion. The flux fusion procedure was originally recommended for both practical and analytical purposes. In the practical sense, the use of flux fusions for the ICP-AES allowed for significant financial savings because much of the required apparatus was already acquired and in use to prepare samples for the wavelength dispersive X-ray fluorescence instrument that was on board the *JOIDES Resolution* at the time. For analytical purposes, flux fusions were recommended over acid digestions for shipboard analyses because acid digestions (1) did not allow for the analysis of Si, due to the volatilization of Si in the presence of HF, (2) did not yield usable results for refractory elements (e.g., Ti, Cr, and Zr)

hosted in minerals that are difficult to dissolve (respectively, rutile, chromite, and zircon), and (3) presented safety concerns with using HF in a shipboard environment.

The geochemical laboratory on board the ship during Leg 199 (Paleogene Equatorial Transect; Lyle, Wilson, Janecek et al., 2002; Quintin et al., 2002) and during many other legs has successfully demonstrated that flux fusion sample preparation produces reliable geochemical data with an acceptable degree of precision and highlighted the utility of using such data for first-order paleoceanographic interpretations. However, whereas the flux fusion scheme results in complete dissolution of all phases (Potts, 1987, and references therein), the use of the lithium metaborate potentially contaminates the laboratory with Li and B, elements of interest to both pore water chemists and igneous geochemists. Although cross contamination has been minimized by maintaining separate inventories of instrument glassware for the ICP-AES, if such a flux fusion-based solution is passed through an ICP-MS, the instrument will be thoroughly, and perhaps permanently, contaminated with Li. Because of the addition of matrix, flux fusion also potentially compromises the analysis of some key trace metals (e.g., Ni, V, Cr, Zn, and rare earth elements) by raising the procedural detection limit.

Thus, in order to extend the element menu and provide a more analytically palatable laboratory environment, the ability to prepare samples using an acid digestion scheme would be desirable. Whereas acid digestions have their limitations, as listed above, a newly advanced microwave-assisted protocol has been developed at Boston University to overcome most of those limitations. The microwave-assisted approach minimizes digestion times, and by using boric acid as part of the reagent cocktail, the formation of insoluble fluorides can be inhibited and Si preserved and thus measured. Overall, the microwave-assisted acid technique with the use of boric acid is a quick and safe method for digesting sediment and perhaps other lithologies that could be used in the shipboard environment.

In this paper, we compare shipboard and shore-based flux fusion results. We also compare shore-based flux fusion results to those derived from microwave-assisted acid digestions. We show that (1) the current shipboard methods are adequate for both shipboard and shore-based sedimentary chemical uses, (2) the microwave-assisted acid technique yields a complete (and HF-safe) digestion, and (3) the microwave-assisted acid digestion holds great potential to be the primary means of digesting sediments on future IODP expeditions. We discuss preliminary results from ODP Leg 206, Site 1256, as it provides an excellent sample suite to compare flux fusion with the newly developed microwave-assisted acid digestion technique and contrast shore-based measurements with the shipboard initial results on Leg 206.

SITE 1256

The sedimentary overburden at Site 1256, in the Guatemala Basin in the eastern equatorial Pacific (Fig. F1), consists of two end-member lithologies, with terrigenous clay in the upper 40 m and biogenic carbonates deeper in the section. The deeper 200-m biogenic carbonate sequence also contains a 4-m-thick laminated diatom mat at ~111 meters below seafloor (mbsf). The carbonates from here to the bottom of the sequence also contain chert nodules. Initial shipboard geochemical results indicate a decrease with depth in the abundance of terrigenous

F1. Location map of ODP Site 1256, Leg 206, p. 11.

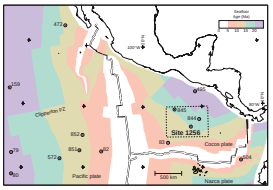

material (with intervals of volcanic ash) into a lithology dominated by calcareous nannofossil ooze, with a large chemical change at the base of the laminated diatom mat at ~115 mbsf. Increased Fe concentrations, manifested by an elevated Fe/Al ratio, indicate a significant metalliferous component near the basement, although the 1-m-thick red-brown oxide-rich sediment layer directly overlying the basalt was not sampled for this study. With a variety of lithologies and sedimentary components, the sediments at Site 1256 provide a suitable sample suite to test the appropriateness of different sample preparation methods for sediments from several different depositional conditions.

SAMPLE PREPARATION

Shipboard Flux Fusion

The *JOIDES Resolution* flux fusion method is detailed in Murray et al. (2000), Quintin et al. (2002), and Wilson, Teagle, Acton, et al. (2003), and is only summarized here. The 28 bulk sediment samples (1 per core) were sampled as a split from the interstitial water squeeze cakes, freeze-dried, and powdered manually with an agate mortar and pestle. Each powdered sample was first ignited as part of the loss on ignition (LOI) analysis to release volatile phases and to fully oxidize all iron to ferric iron. Each ignited sample was mixed with $LiBO_2$ flux in a 1:4 sample/flux ratio in a Pt-Au crucible coated with a LiBr wetting agent to avoid sticking and heated at 900°C in a NT-2100 Bead Sampler furnace for 3 min. Upon subsequent cooling, the now glass bead sample was dissolved in 50 mL of 10% HNO_3 to yield a 1000-fold dilution. Once the glass bead was completely dissolved, the aqueous solution was filtered and further diluted 4000-fold for instrumental uptake.

Shore-Based Flux Fusion

At Boston University, we randomly selected 35 samples from the 100 sample shore-based set. We sampled from the same squeeze cake split that was used for the shipboard analyses. The general procedures were similar to those used during the cruise, with three exceptions. First, we did not perform an LOI analysis because it is not recommended for biogenic-rich sediments (Murray et al., 2000). The LOI comprises a significant portion of the total mass of the sample, and thus potentially introduces error in the total and often compromises the alkali results due to their inadvertent loss via volatilization. Considering that carbonate sediments are an important portion of the sample set, we bypassed the LOI analysis and thus maintained procedural consistency through all lithologies. Thus, when comparing the shipboard and shore-based results, we calculated all concentrations on an anhydrous basis. Second, on board the *JOIDES Resolution,* the use of Pt-Au crucibles required a wetting agent, whereas the use of graphite crucibles at Boston University does not. Third, the furnace temperature was increased to 1050°C and the fusing time increased from 3 to 12 min. The ovens used in the two laboratories are fundamentally different, with the *JOIDES Resolution* facility being a special unit with a rapid temperature rise whereas at Boston University we use a standard muffle furnace.

Shore-Based Acid Digestion

All 100 samples for the shore-based acid digestion sample set were acquired from the interstitial water squeeze cakes that were taken at a higher resolution (2 per core). Some of these samples were also splits of the shipboard samples. The objectives for the higher resolution sample set were to capture the complete chemical variability at Site 1256 and to better characterize the entire sediment sequence, and the scientific significance of these results will be presented elsewhere. Only 10 items (samples, standards, blanks, etc.) can be processed per batch when using the microwave system; therefore, 12 batches were required to digest all samples, with multiple replicates, standards, and blanks distributed between the 12 batches.

Approximately 50 mg of freeze-dried, powdered sample was placed into a microwave digestion vessel that contained a mixture of HNO_3, HCl, and HF (6:2:2 mL, respectively). The vessel was then tightly sealed and placed into a Milestone Ethos-Plus microwave system (Milestone Inc., Shelton Connecticut, USA). The first three step-wise temperature settings consisted of ramping to 160°C over 12 min, then to 210°C over 8 min, and finally holding constant at 210°C for 30 min. The vessels vented for 30 min and cooled to <50°C, whereby they were opened and 0.5 mL of 30% hydrogen peroxide (H_2O_2) and 10 mL of 5% boric acid (H_3BO_3) were added immediately. For samples with a higher organic content (approximately >0.5 wt% C_{org}), 1 mL of H_2O_2 was used. Vessels were immediately resealed and placed back into the microwave for a second digestion. This second digestion consisted of a ramp time of 8 min to 160°C, and the temperature was held constant at 160°C for an additional 7 min. The vessels were again vented for 30 min and cooled to 50°C prior to opening. Each sample was then transferred to a preweighed bottle and brought to a total of 50 g with deionized water (Milli-Q, 18 MΩ) for a 1000-fold dilution. We selected a 1000-fold dilution factor to ensure a better signal-to-noise ratio for the lower concentration trace elements in carbonates while also maintaining a low amount of total dissolved solids (TDS). To minimize the potential for clogging of the nebulizer on the ICP-AES with this 1.1% TDS solution, we used a Teflon nebulizer and spray chamber. We recommend a total 6000-fold dilution factor for the more commonly used Meinhardt concentric glass nebulizers. However, use of the Teflon system we employed also provides the additional benefit of preventing enhanced consumption of glass nebulizers and spray chambers.

INSTRUMENT MEASUREMENTS

Both shipboard and shore-based samples were measured with Jobin-Yvon (JY) ICP-AES instruments. The JY2000 instrument on the *JOIDES Resolution* employs a monochrometer, enabling the sequential measurement of individual wavelengths while rapidly scanning through the spectrum. The JY ULTIMA-C instrument at Boston University has the capability to measure both individual and multiple wavelengths simultaneously, as it employs a monochrometer as well as a polychrometer. Thus, the shore-based protocol measured most major elements (Si, Al, Ti, Fe, Mn, Ca, and Mg) and the trace element Sr on the polychrometer with other major and trace elements (Na, K, Ba, Cr, Ni, Sc, V, and Zr) on the monochrometer. The same wavelengths for each element were measured on both instruments. For the monochrometers, the optical focal

length on the Boston University instrument (1 m) is also longer than that on the *JOIDES Resolution* (0.6 m), allowing better resolution of spectra, although this has not shown to be a handicap for the shipboard instrument.

Quality Assurance and Quality Control

The standard reference materials (SRMs) used in calibrating each ICP-AES were slightly different between the shipboard and shore-based protocols. The shipboard SRMs included BCSS-1 (marine mud), BHVO-2 (Hawaiian basalt), JCh-1 (Japanese chert), JLs-1 (Japanese limestone), NIST-1c (argillaceous limestone), and MAG-1 (marine mud) for a six-point calibration curve, with SCo-1 (Cody shale) being measured as an unknown item to check accuracy and consistency between analytical runs (Shipboard Scientific Party, 2003). The shore-based SRMs consisted of MAG-1, SCo-1, JA-2 (Japanese andesite), and BCSS-1 as a four-point calibration curve for the upper terrigenous-rich sequence. For the carbonate-rich samples we used a four-point calibration curve consisting of JLs-1, MAG-1, and two gravimetrically mixed standards of 80% JLs–20% MAG-1, and 60% JLs–40% MAG-1. Constructing these mixed standards enabled a better matrix match and a more appropriate concentration range for the calibration. At times JCh-1 was used in the calibration to also help constrain the silica-rich samples. NIST-1c was used as an accuracy check and was within one standard deviation of the published uncertainty (Table **T1**). Furthermore, a composite sample from Site 1256 (termed "EEP") was used at Boston University to monitor consistency between runs.

The analytical uncertainties, presented as precision, for the shore-based and shipboard procedures (Table **T2**) quantify the sum of the uncertainties due to both instrument variability and the sample preparation process. Precision was calculated by percent of variation associated with a random sample that had been prepared and measured separately three times. Comparing shipboard flux fusions with flux fusions performed at Boston University, the precision improved significantly, with Boston University being better than 3% of the respectively measured values for Si, Al, Ti, Fe, Mg, and Ba. Elements that were not reported during the cruise (P and Zr) as a result of poor uncertainty (>30% of the measured values) are both within 4% of the measured value from shore-based analysis. The uncertainty of the alkali elements (Na and K) shipboard is >20% of the measured values, whereas shore-based precisions are better than 3% of the measured values. Some of the high shipboard uncertainty may be caused by the LOI procedure that was performed only at sea, as well as by other reasons such as the physical motion of the ship (see discussion in Quintin et al., 2002). Trace elements such as Cr, Ni, and V are often difficult to measure in carbonates, due to their low concentrations, and thus procedures on board the ship probably approached the procedural detection limit. However, at Boston University, we adjusted the calibration curve to suit carbonate-rich sediments and prepared the samples in a cleaner and more stable environment than aboard the *JOIDES Resolution*.

Importantly, the difference between flux fusions at Boston University and microwave-assisted acid digestions is minor. The microwave typically yielded precision better than 3% of the measured values for all elements, including Cr, Ni, V, and Zr. As will be discussed below, this agreement between the flux fusion and the acid digestion, even for elements that are traditionally difficult to dissolve, demonstrates the abil-

T1. Accuracy of reference material NIST-1c in shore-based measurements, p. 17.

T2. Reproducibility of each digestion method, p. 18.

ity of using microwave-assisted digesting systems to prepare samples for ICP analyses.

SHORE-BASED FLUX VS. SHORE-BASED MICROWAVE ACID DIGESTION

Approximately 35 samples were randomly selected from throughout Site 1256 and were prepared at Boston University by both the flux fusion method and the microwave-assisted acid digestion method. All samples were measured by ICP-AES for major elements (Si, Al, Ti, Fe, Mn, Ca, Mg, Na, K, and P) and selected trace elements (Ba, Sr, Cr, Ni, Sc, V, and Zr). As mentioned earlier, both the flux fusion and acid digestion analyses were calibrated with the same standard reference materials.

The analyses from each preparation are in good agreement (Fig. **F2;** Table **T3**). For each element, the microwave-assisted acid digestions show a complete digestion as the concentrations fall on or very near to the 1:1 line with the concentrations produced by flux fusions. Importantly, the refractory elements, such as Ti and Zr, also fall on the 1:1 line, signifying that the acid digestions can achieve a complete digestion when using HF in a pressurized microwave for an extensive period of time, which allows for ample conditions to dissolve refractory minerals in these sediments.

Boric acid was added in the microwave-assisted digestion method to prevent the formation of insoluble fluorides and to inhibit the volatilization of Si. A robust 1:1 relationship between flux fusions and microwave-assisted acid digestions for Ca and Al also demonstrates the usefulness of the boric acid and the inhibition of insoluble fluorides. If fluoride precipitation occurred, Ca and Al concentrations are likely to have fallen below the 1:1 line. Moreover, the 1:1 relationship for Si between shipboard flux and shore-based acid digestions is also tight (r^2 = 0.982), indicating that the small amount of Si lost by volatilization (even in the presence of the boric acid, and evidenced by the slope of 0.936) is predictable and minor in extent. Overall, the descriptive statistics in Table **T4** indicate a strong correlation within the analytical uncertainties.

While most elements show excellent correlation and regression slopes very near unity, Ni and Cr, however, present correlation coefficients better than 0.95 yet yield regression slope values 10%–15% smaller than unity (Table **T4**). The variability observed with Ni and Cr potentially reflects the variability in the flux fusions, as these elements are less precisely determined by flux methods at these low concentrations than by acid digestion (Table **T1**).

In summary, the comparison between flux fusions and microwave-assisted acid digestions demonstrates that with the addition of boric acid

1. HF can be used to completely digest most sediment types, ranging from terrigenous-rich to biogenic-rich, without compromising elements that are typically lost to fluoride precipitation;
2. the removal of HF (i.e., volatilization during dry downs) is not necessary, as boric acid neutralizes any excess HF for safely handling the sample solutions and provides a solution matrix suitable for instrument uptake; and
3. allows for Si and difficult trace elements to be accurately measured.

F2. Flux vs. microwave-assisted acid digestions, p. 12.

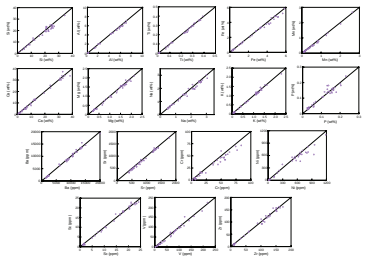

T3. Results from flux fusion and microwave acid digestions, p. 19.

T4. Shore-based flux fusion vs. microwave-assisted acid digestions, p. 22.

These results indicate the usefulness and practicality of using microwave-assisted acid digestions in future IODP laboratories.

SHIPBOARD VS. SHORE-BASED DIGESTIONS

Shipboard Flux Fusion vs. Shore-Based Flux Fusion

The results from shipboard flux fusions and those from shore-based flux fusions show strong correlations (r^2 = ~0.95) for all elements, except for Mn, Ba, Sr, and Cr (Fig. F3). Most major elements reflect a systemic offset, whereby shipboard data are greater than shore-based data. This offset can be attributed to the fact that LOI was performed on the carbonate-rich shipboard samples and that the major elements were normalized with regard to Ca, such that the CaO concentrations were consistent with the amount required to balance the inorganic carbon (as $CaCO_3$) determined by coulometry (Shipboard Scientific Party, 2003). Chromium is the only element with a significant difference between the analyses and is explained by the difficulty of precisely and accurately measuring trace elements in carbonates in the shipboard environment. Shore-based results also reflect Cr concentrations that are typical of biogenic-rich sediment, suggesting that the shore-based acid digestions are more accurate than shipboard results.

F3. Shipboard vs. shore-based flux fusion digestions, p. 14.

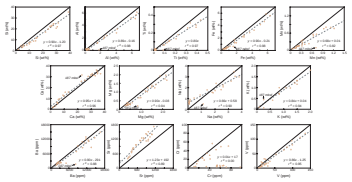

Shipboard Flux Fusion vs. Shore-Based Microwave-Assisted Acid Digestion

Microwave-assisted acid digestion results are listed in Table T5 and shipboard results are reported in the Leg 206 *Initial Reports* volume (Wilson, Teagle, Acton, et al., 2003). The depth profiles of shipboard flux fusions and high resolution shore-based microwave acid digestions exhibit strong correlation (r^2 > 0.95) and display similar downhole trends for all elements, except for Mn and Cr (Table T6; Fig. F4). Systematic offsets however, as indicated by the regression slopes, highlight the differences between shipboard and shore-based analytical procedures and the corrections applied to shipboard data, in comparison to the more accurate shore-based data, as discussed above. The shore-based microwave acid digestions also reflect the higher resolution sampling. Nonetheless, both data sets exhibit the same lithological and chemical characteristics with depth.

T5. Results from microwave acid digestions, p. 23.

T6. Shipboard flux fusion vs. shore-based microwave-assisted acid digestions, p. 26.

F4. Depth profiles of major and trace elements, p. 15.

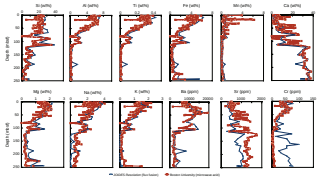

More importantly, elemental ratios, such as Ba/Ti, Al/Ti, and Fe/Al, that were used in the *Initial Reports* (Wilson, Teagle, Acton, et al., 2003) for paleoceanographic interpretations are consistent with the shore-based acid digestions (Fig. F5). This consistency suggests that the shipboard first-order paleoceanographic interpretations are robust and that the acid digestion protocol successfully provides high-resolution chemical data.

F5. Depth profiles of Ba/Ti, Al/Ti, and Fe/Al ratios, p. 16.

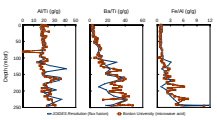

CONCLUSIONS

As previous shipboard sample preparation procedures recommended using flux fusions to dissolve sediment for ICP analyses (Murray et al., 2000; Quintin et al., 2002), the newly developed microwave-assisted acid digestion procedure could enable shipboard scientists to expand the element menu and broaden initial geochemical interpretations

based on either ICP-ES or ICP-MS analyses in future IODP laboratories. By comparing samples prepared by flux fusion and microwave-assisted acid digestion, the microwave acid digestion technique demonstrates its ability to achieve a complete digestion. With the addition of boric acid, HF can be used safely, Si can be directly measured, and key elements that are typically compromised by the formation of insoluble fluorides can be preserved. The shipboard flux to shore-based acid digestion comparison demonstrates that the current shipboard procedures are more than adequate to produce quick and accurate geochemical results for first-order geochemical interpretations. As retooling of analytical procedures and analytical capabilities on future expeditions are being considered, microwave acid digestions could be used to digest sediments.

ACKNOWLEDGMENTS

We thank the Leg 206 Science Party for their patience and support of our enthusiastic studies of what the solid-rockers referred to as the sediment "overburden." In reality, of course, it is their basalt that exists primarily to hold up the sediment. We also extend gratitude to Damon Teagle, David Wray, and an anonymous reviewer for their comments and revisions that helped make this manuscript better. This research used samples and/or data provided by the Ocean Drilling Program (ODP). The ODP is sponsored by the U.S. National Science Foundation (NSF) and participating countries under management of Joint Oceanographic Institutions (JOI), Inc. This work was funded by a JOI-U.S. Science Support Program (USSSP) grant to R.W. Murray and C.L. Ziegler and NSF grant EAR 02-33712 that helps support the Analytical Geochemistry facilities at Boston University. Many thanks to April Azouz and Stephiane Frana for their assistance with sample preparations, and Louise Bolge for her gracious help with the ICP instrumentation.

REFERENCES

Christie, D.M., Pedersen, R.B., Miller, D.J., et al., 2001. *Proc. ODP, Init. Repts.,* 187: College Station, TX (Ocean Drilling Program). **doi:10.2973/odp.proc.ir.187.2001**

Lyle, M., Wilson, P.A., Janecek, T.R., et al., 2002. *Proc. ODP, Init. Repts.,* 199: College Station, TX (Ocean Drilling Program). **doi:10.2973/odp.proc.ir.199.2002**

Murray, R.W., Miller, D.J., and Kryc, K.A., 2000. Analysis of major and trace elements in rocks, sediments, and interstitial waters by inductively coupled plasma–atomic emission spectrometry (ICP-AES). *ODP Tech. Note,* 29 [Online]. Available from World Wide Web: <**http://www-odp.tamu.edu/publications/tnotes/tn29/INDEX.HTM**>. [Cited 2005-05-02]

Potts, P.J., 1987. *A Handbook of Silicate Rock Analysis:* Glasgow and London (Blackie).

Quintin, L.L., Faul, K.L., Lear, C., Graham, D., Peng, C., Murray, R.W., and Shipboard Scientific Party, 2002. Geochemical analysis of bulk marine sediment by inductively coupled plasma–atomic emission spectroscopy on board the *JOIDES Resolution*. *In* Lyle, M., Wilson, P.A., Janecek, T.R., et al., *Proc. ODP, Init. Repts.,* 199: College Station, TX (Ocean Drilling Program), 1–14. **doi:10.2973/odp.proc.ir.199.107.2002**

Tréhu, A.M., Bohrmann, G., Rack, F.R., Torres, M.E., et al., 2003. *Proc. ODP, Init. Repts.,* 204: College Station, TX (Ocean Drilling Program). **doi:10.2973/odp.proc.ir.204.2003**

Shipboard Scientific Party, 2003. Explanatory notes. *In* Wilson, D.S., Teagle, D.A.H., Acton, G.D., et al., *Proc. ODP, Init. Repts.,* 206: College Station, TX (Ocean Drilling Program), 1–94. **doi:10.2973/odp.proc.ir.206.102.2003**

Wilson, D.S., Teagle, D.A.H., Acton, G.D., et al, 2003. *Proc. ODP, Init. Repts.,* 206: College Station, TX (Ocean Drilling Program). **doi:10.2973/odp.proc.ir.206.2003**

Figure F1. Location map of Site 1256, Leg 206. From Wilson, Teagle, Acton, et al. (2003). FZ = Fracture Zone.

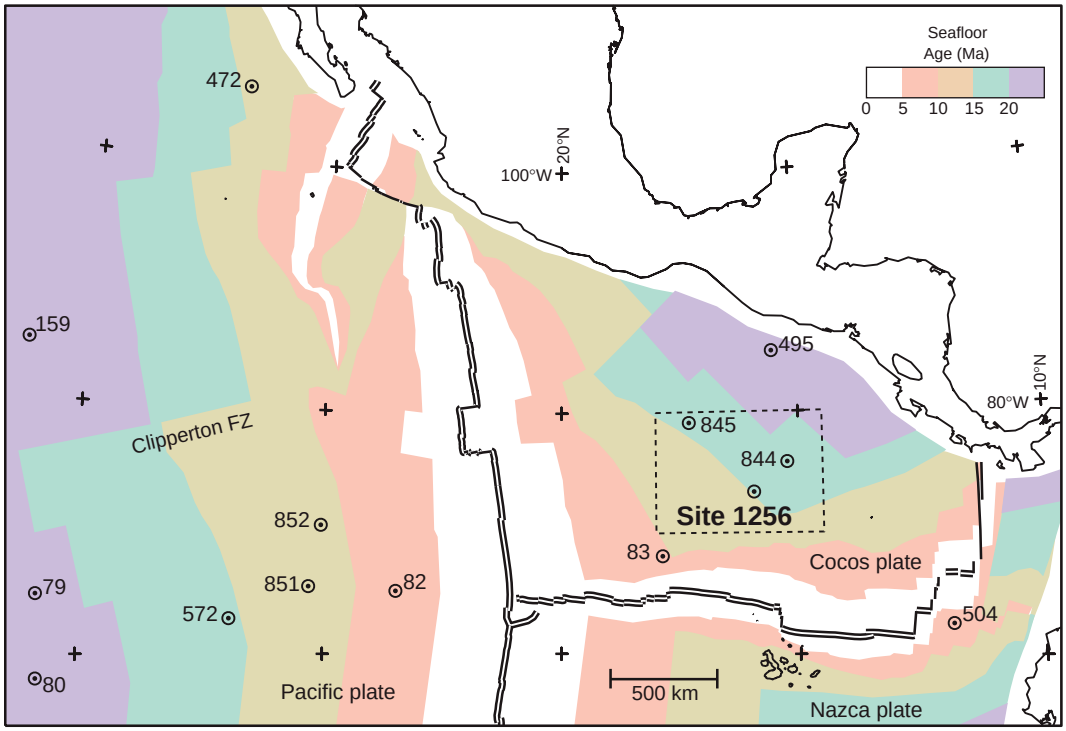

Figure F2. Comparison of concentrations between flux and microwave-assisted acid digestions at Boston University. The solid diagonal line is a 1:1 line, not a linear regression of the data. X-axis = microwave-assisted acid digestions, y-axis = flux fusion digestions. (**Figure shown on next page.**)

Figure F2 (continued). (Caption shown on previous page.)

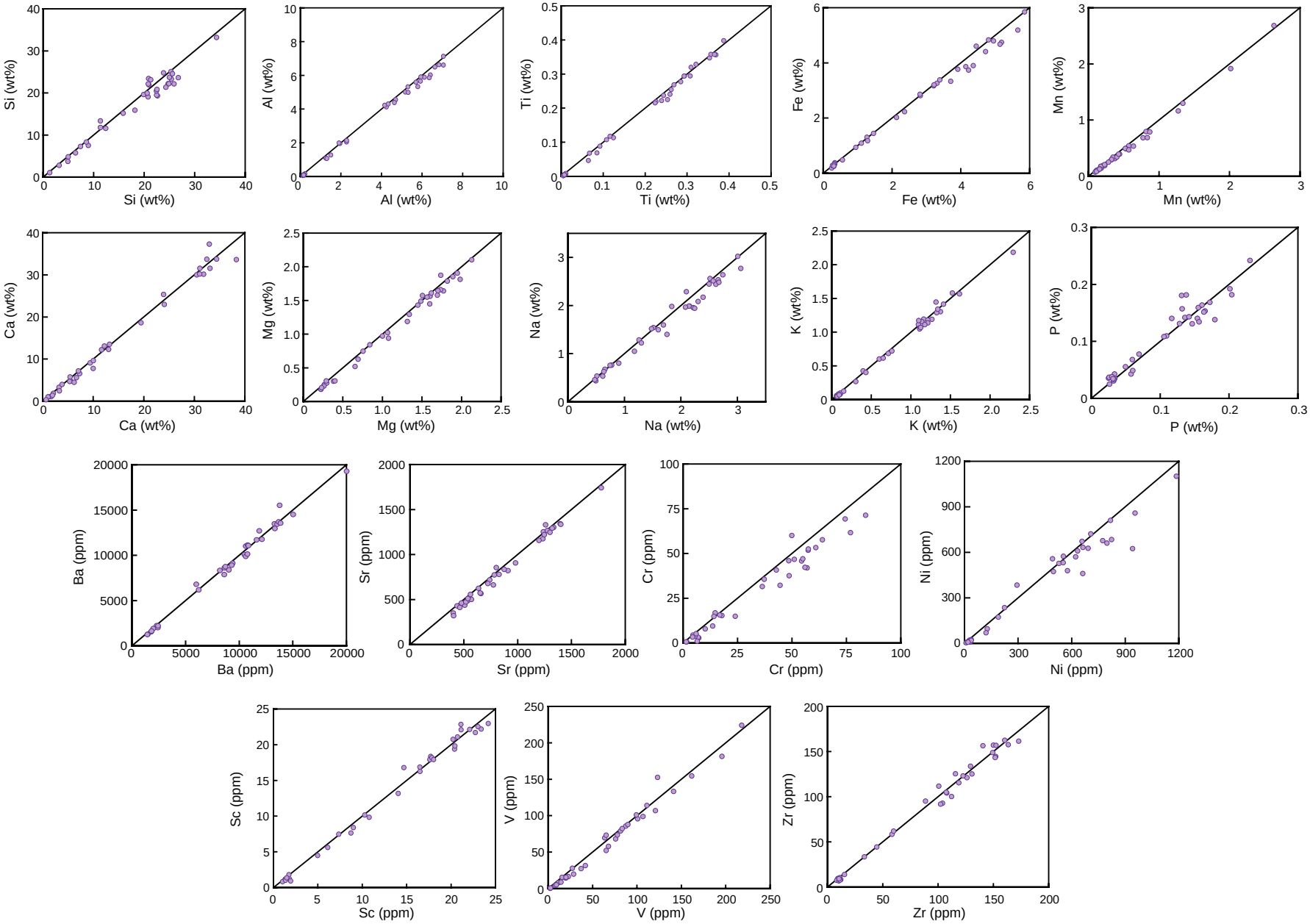

Figure F3. Comparison of concentrations between shipboard and shore-based flux fusion digestions. Solid line is a 1:1 line. Dashed line represents linear regression of data. X-axis = shore-based flux fusion digestions, y-axis = shipboard flux fusion digestions.

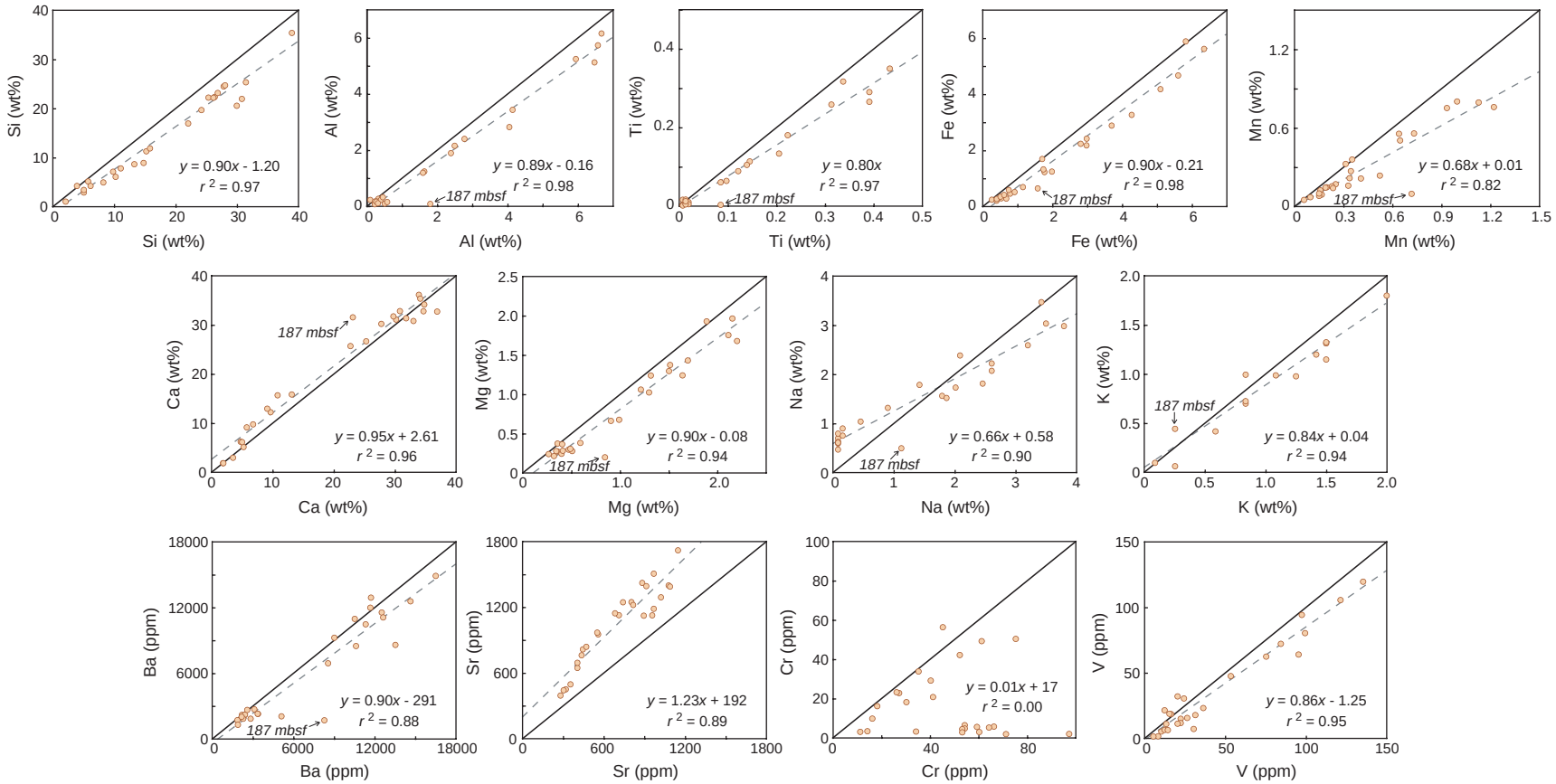

Figure F4. Depth profiles of major and trace elements. Circles = shipboard measurements, squares = shore-based measurements.

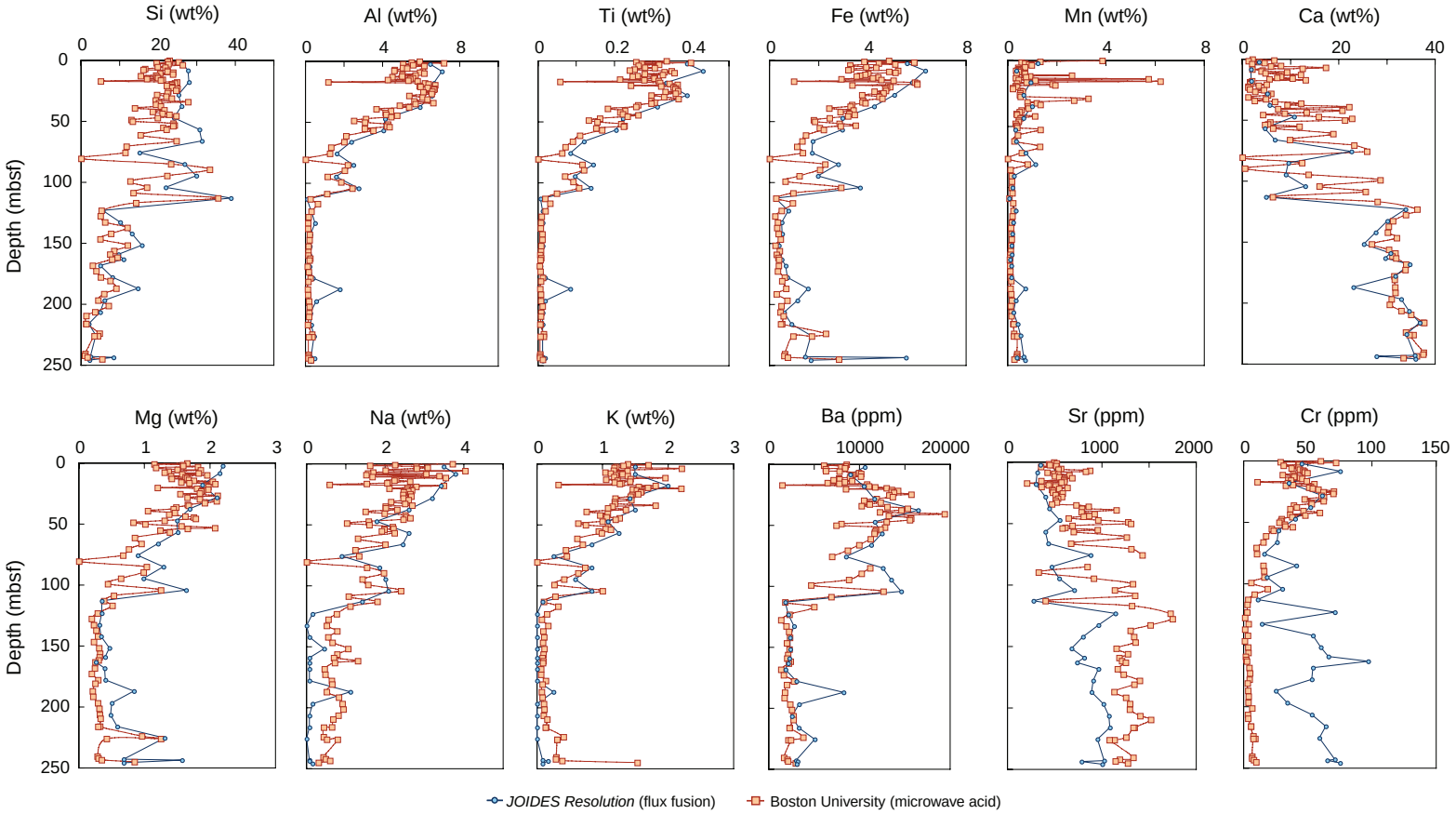

Figure F5. Depth profiles of shipboard flux (squares) and shore-based microwave acid (circles) results of Ba/Ti, Al/Ti, and Fe/Al ratios (g/g).

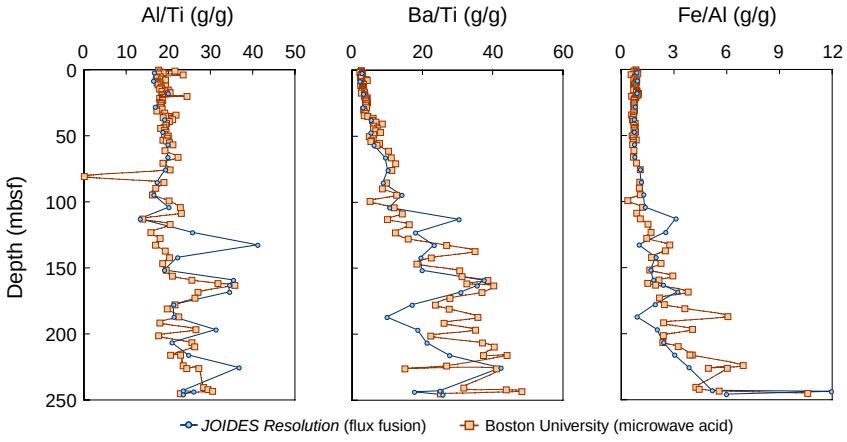

Table T1. Accuracy of standard reference material NIST-1c in shore-based (flux and microwave-assisted digested) measurements.

Element	Published value	Measured value ($N = 6$)
Major element oxide (wt%):		
SiO_2	6.84 ± 0.08	6.78 ± 0.24
Al_2O_3	1.30 ± 0.03	1.28 ± 0.02
TiO_2	0.070 ± 0.010	0.069 ± 0.002
Fe_2O_3	0.55 ± 0.03	0.56 ± 0.02
MnO	0.025 ± 0.005	0.021 ± 0.001
CaO	50.3 ± 0.3	50.4 ± 1.0
MgO	0.42 ± 0.04	0.39 ± 0.01
Na_2O	0.020 ± 0.010	0.020 ± 0.001
K_2O	0.28 ± 0.01	0.29 ± 0.01
P_2O_5	0.04 ± 0.01	0.038 ± 0.001
Trace element (ppm):		
Ba	NR	56.3 ± 1.5
Sr	254 ± 42	257 ± 8
Cr	NR	11.7 ± 0.3
Ni	NR	8.91 ± 0.45
Sc	NR	1.47 ± 0.04
V	NR	10.4 ± 0.4
Zr	NR	35.1 ± 1.4

Notes: Error reported as 1σ. NR = not reported.

Table T2. Reproducibility of each digestion method.

Element	Shipboard Flux Fusion (%) (*N* = 6)	Boston University Flux Fusion (%) (*N* = 4)	Boston University Microwave (%) (*N* = 8)
Major element (wt%):			
Si	3.4	1.9	1.9
Al	5.0	2.6	1.9
Ti	5.8	3.0	2.5
Fe	7.1	2.7	2.2
Mn	2.9	1.4	2.1
Ca	1.5	2.5	1.8
Mg	3.9	2.5	2.0
Na	>20	1.7	1.2
K	>20	2.8	2.0
P	>30 (NR)	4.1	2.0
Trace elements (ppm):			
Ba	6.9	1.2	1.9
Sr	2.7	2.3	1.8
Cr	>20	4.5	3.2
Ni	13.1	4.5	3.0
Sc	NR	3.3	2.4
V	10.2	3.1	3.0
Zr	>30 (NR)	4.0	3.0

Notes: Precision reported as percent of 1σ standard deviation of the mean concentration. NR = not reported in Leg 206 *Initial Reports* (Wilson, Teagle, Acton, et al., 2003).

Table T3. Results from the Boston University flux fusion and microwave acid digestions. (Continued on next two pages.)

Core, section, interval (cm)	Depth (mbsf)	Major elements (wt%)															
		Si		Al		Ti		Fe		Mn		Ca		Mg		Na	
		Flux	Microwave	Flux	Microwave	Flux	Microwave	Flux	Microwave	Flux	Microwave	Flux	Microwave	Flux	Microwave	Flux	Microwave
206-1256B-																	
1H-1, 145–150	1.45	25.16	25.25	7.02	7.17	0.386	0.400	5.84	5.87	0.563	0.555	1.56	1.25	1.50	1.58	1.68	1.61
1H-2, 70–75	2.20	22.48	19.50	5.15	5.05	0.267	0.271	4.70	4.44	0.765	0.696	3.10	3.45	1.69	1.59	3.05	2.79
1H-4, 70–75	5.20	19.76	19.79	5.29	5.03	0.283	0.280	4.34	3.93	0.825	0.700	9.86	7.95	1.48	1.50	2.14	2.00
2H-1, 142–147	7.52	18.02	16.09	4.66	4.60	0.242	0.239	3.19	3.20	0.430	0.405	12.90	12.46	1.33	1.30	1.50	1.56
2H-2, 0–75	8.27	24.63	22.36	6.38	6.07	0.352	0.349	5.64	5.22	0.365	0.325	1.98	2.03	1.97	1.82	2.99	3.04
2H-2, 145–150	9.02	25.78	22.32	6.08	5.92	0.320	0.331	4.78	4.86	0.524	0.500	3.71	4.13	1.59	1.57	1.59	1.51
3H-3, 145–150	20.05	25.24	23.47	6.32	5.90	0.258	0.243	3.69	3.36	2.007	1.929	1.80	1.56	1.31	1.20	2.29	2.10
3H-4, 70–75	20.80	20.78	22.13	5.91	5.95	0.308	0.322	4.93	4.82	0.318	0.309	5.37	5.00	1.81	1.80	2.65	2.55
3H-5, 70–75	22.30	20.73	23.59	6.80	6.67	0.355	0.360	5.17	4.77	0.196	0.204	1.00	1.20	1.73	1.89	2.50	2.58
3H-5, 145–150	23.05	23.71	24.94	7.02	6.65	0.367	0.358	5.12	4.70	0.222	0.201	0.92	1.18	1.88	1.86	2.49	2.46
4H-1, 145–150	26.55	24.77	22.37	6.60	6.53	0.364	0.359	4.43	4.63	0.512	0.506	3.18	2.62	2.12	2.11	2.73	2.66
4H-2, 145–150	28.05	22.33	19.66	5.76	5.37	0.292	0.296	4.20	3.76	0.562	0.481	5.27	5.90	1.76	1.65	2.61	2.46
4H-5, 145–150	32.55	20.64	19.26	5.67	5.63	0.291	0.296	3.89	3.79	2.619	2.697	5.21	4.84	1.94	1.92	2.66	2.50
4H-7, 71–76	34.81	20.47	20.13	5.89	5.69	0.306	0.296	4.13	3.89	1.264	1.176	7.18	6.70	1.73	1.67	2.13	2.00
5H-2, 145–150	37.55	22.30	20.62	5.27	5.36	0.260	0.256	3.29	3.29	0.807	0.809	9.27	9.27	1.44	1.44	2.08	2.30
5H-4, 145–150	40.55	24.17	21.54	4.61	4.42	0.252	0.227	3.37	3.41	0.627	0.549	6.92	7.37	1.59	1.46	2.07	1.98
5H-6, 145–150	43.55	22.40	21.02	4.21	4.17	0.224	0.221	3.20	3.23	0.338	0.352	12.07	13.27	1.61	1.62	2.56	2.53
6H-5, 145–150	51.55	24.86	23.88	4.12	4.27	0.222	0.217	2.80	2.84	0.318	0.309	6.56	5.73	1.56	1.56	2.38	2.19
6H-7, 65–70	53.75	26.63	23.81	4.30	4.35	0.238	0.224	2.80	2.89	0.394	0.355	6.07	4.64	1.69	1.66	2.20	1.97
7H-5, 145–150	61.05	15.70	15.36	2.24	2.09	0.106	0.109	1.44	1.47	0.420	0.405	19.33	18.80	0.83	0.85	1.25	1.30
8H-2, 145–150	66.05	25.45	24.72	1.92	2.00	0.091	0.090	1.25	1.33	0.276	0.264	9.88	9.82	1.07	0.95	1.83	2.00
8H-5, 145–150	70.55	12.25	11.74	1.47	1.32	0.084	0.071	1.09	1.12	1.330	1.311	23.92	23.14	0.75	0.76	1.29	1.24
10H-2, 145–150	85.05	21.17	23.29	2.25	2.18	0.123	0.115	2.34	2.26	0.860	0.800	11.49	12.36	1.06	1.03	1.47	1.53
10H-5, 145–150	89.55	34.20	33.34	1.87	2.03	0.115	0.120	2.11	2.05	0.115	0.111	0.54	0.50	0.99	0.98	2.23	1.96
11H-2, 145–150	94.55	20.68	22.31	1.22	1.13	0.066	0.070	1.27	1.21	0.175	0.159	13.09	13.68	0.68	0.64	1.74	1.41
12H-5, 145–150	108.55	11.21	13.55	1.28	1.11	0.063	0.048	0.93	0.96	0.164	0.187	23.80	25.53	0.65	0.53	1.16	1.06
14H-5, 145–150	127.55	4.83	4.99	0.14	0.15	0.009	0.009	0.23	0.22	0.167	0.187	32.34	33.89	0.21	0.19	0.50	0.55
15H-5, 145–150	137.05	11.20	11.98	0.13	0.12	0.006	0.006	0.25	0.30	0.131	0.130	31.70	30.31	0.26	0.26	0.76	0.78
16H-2, 145–150	142.05	8.79	7.71	0.19	0.21	0.009	0.010	0.32	0.36	0.151	0.141	30.33	30.15	0.29	0.29	0.61	0.55
17H-5, 145–150	156.05	8.40	8.52	0.14	0.14	0.006	0.007	0.32	0.41	0.105	0.117	30.93	30.38	0.28	0.32	0.73	0.77
18H-1, 95–100	159.05	7.25	7.44	0.13	0.13	0.005	0.005	0.29	0.28	0.097	0.100	32.96	31.72	0.37	0.31	0.64	0.69
20X-2, 145–150	168.15	3.02	2.95	0.10	0.10	0.003	0.004	0.31	0.37	0.086	0.085	34.28	33.93	0.25	0.24	0.48	0.45
20X-5, 145–150	172.65	4.77	3.90	0.14	0.15	0.005	0.006	0.29	0.33	0.102	0.097	38.17	33.77	0.21	0.19	0.46	0.47
22X-5, 145–150	191.45	6.27	5.90	0.12	0.12	0.006	0.007	0.29	0.28	0.148	0.140	30.98	31.71	0.22	0.22	0.89	0.82
25X-2, 140–145	215.90	1.17	1.24	0.13	0.13	0.006	0.006	0.54	0.51	0.219	0.217	32.83	37.48	0.39	0.32	0.62	0.64

Notes: Data overspecified for calculation purposes. See text for discussion of true analytical precision.

Table T3 (continued).

Core, section, interval (cm)	Depth (mbsf)	Major elements (wt%)				Trace elements (ppm)									
		K		P		Ba		Sr		Cr		Ni		Sc	
		Flux	Microwave	Flux	Microwave	Flux	Microwave	Flux	Microwave	Flux	Microwave	Flux	Microwave	Flux	Microwave
206-1256B-															
1H-1, 145–150	1.45	1.37	1.31	0.154	0.161	8,127	8,419	431	437	83.46	71.78	289.4	389.3	24.12	23.07
1H-2, 70–75	2.20	1.15	1.20	0.146	0.132	8,543	7,949	502	445	56.63	42.30	813.8	815.9	20.31	19.48
1H-4, 70–75	5.20	1.13	1.17	0.127	0.132	6,159	6,267	556	565	55.64	42.60	769.7	682.0	17.62	18.45
2H-1, 142–147	7.52	1.09	1.12	0.116	0.142	10,410	10,155	904	828	54.08	46.23	489.0	562.1	16.43	16.37
2H-2, 0–75	8.27	1.32	1.30	0.203	0.183	9,311	9,209	457	420	50.70	47.15	658.6	465.0	23.31	22.28
2H-2, 145–150	9.02	1.26	1.20	0.131	0.158	9,224	8,992	527	492	54.68	47.45	573.0	484.0	22.02	22.23
3H-3, 145–150	20.05	2.28	2.20	0.135	0.143	8,969	8,467	395	357	44.21	32.57	618.3	575.6	13.98	13.28
3H-4, 70–75	20.80	1.31	1.46	0.164	0.154	13,230	13,554	630	633	57.11	52.14	629.7	613.6	20.65	21.19
3H-5, 70–75	22.30	1.52	1.59	0.162	0.153	13,470	13,524	472	469	60.66	53.63	659.0	637.4	21.04	22.95
3H-5, 145–150	23.05	1.60	1.58	0.171	0.170	13,607	13,780	512	482	63.65	58.05	703.2	726.5	22.66	21.81
4H-1, 145–150	26.55	1.40	1.43	0.130	0.182	13,788	13,643	563	508	74.07	69.67	936.9	629.9	22.95	22.63
4H-2, 145–150	28.05	1.20	1.19	0.178	0.139	12,045	11,851	653	575	49.61	60.40	550.1	578.8	20.35	19.92
4H-5, 145–150	32.55	1.09	1.18	0.229	0.243	10,538	11,100	532	520	76.54	62.05	1,333.4	940.9	20.14	20.84
4H-7, 71–76	34.81	1.21	1.15	0.160	0.165	13,250	13,048	733	725	57.19	52.87	819.1	689.6	21.05	22.18
5H-2, 145–150	37.55	1.33	1.35	0.153	0.141	14,956	14,591	821	787	42.52	41.18	654.2	677.0	17.54	18.01
5H-4, 145–150	40.55	1.10	1.08	0.155	0.136	19,939	19,369	776	782	48.18	46.36	793.8	665.1	17.77	18.29
5H-6, 145–150	43.55	1.10	1.06	0.141	0.145	13,694	15,598	794	863	36.95	35.95	688.0	631.6	14.60	16.88
6H-5, 145–150	51.55	1.12	1.08	0.200	0.194	11,796	12,782	716	685	36.06	31.95	951.3	863.3	16.42	16.97
6H-7, 65–70	53.75	1.17	1.12	0.137	0.183	11,547	11,790	645	580	48.40	37.98	1,182.4	1,106.3	17.96	18.02
7H-5, 145–150	61.05	0.59	0.61	0.108	0.111	10,711	11,204	1,233	1,261	14.35	17.16	493.5	478.7	8.92	8.50
8H-2, 145–150	66.05	0.71	0.70	0.049	0.057	10,534	9,953	767	670	23.60	15.28	524.9	531.8	7.65	7.73
8H-5, 145–150	70.55	0.39	0.43	0.068	0.079	8,551	8,687	1,327	1,309	13.22	9.83	548.6	537.2	6.04	5.72
10H-2, 145–150	85.05	0.75	0.73	0.104	0.110	10,786	11,156	868	844	13.81	15.18	219.6	240.3	10.20	10.26
10H-5, 145–150	89.55	0.64	0.63	0.057	0.044	10,703	10,211	398	328	17.48	15.70	185.6	178.7	10.50	9.95
11H-2, 145–150	94.55	0.42	0.41	0.059	0.069	8,643	8,821	974	914	16.48	16.00	123.2	101.0	7.27	7.56
12H-5, 145–150	108.55	0.30	0.28	0.059	0.050	5,923	6,888	1,390	1,350	9.83	8.27	116.1	75.0	4.90	4.80
14H-5, 145–150	127.55	0.05	0.07	0.024	0.037	1,395	1,349	1,770	1,749	1.27	0.99	23.4	26.2	1.24	1.28
15H-5, 145–150	137.05	0.10	0.09	0.025	0.026	2,324	2,208	1,314	1,301	1.04	0.99	33.7	28.8	1.72	1.50
16H-2, 145–150	142.05	0.10	0.11	0.031	0.032	2,235	2,316	1,254	1,338	6.87	3.13	31.4	23.9	1.66	1.90
17H-5, 145–150	156.05	0.08	0.09	0.033	0.044	2,344	2,090	1,269	1,274	6.54	3.57	29.0	15.6	1.41	1.43
18H-1, 95–100	159.05	0.08	0.08	0.025	0.038	1,912	1,986	1,227	1,184	6.12	1.41	5.0	9.2	1.22	1.18
20X-2, 145–150	168.15	0.05	0.06	0.029	0.039	1,362	1,335	1,191	1,165	5.15	4.24	24.7	21.2	0.95	0.93
20X-5, 145–150	172.65	0.06	0.06	0.033	0.036	1,714	1,638	1,241	1,228	4.18	4.73	33.4	24.1	1.28	1.12
22X-5, 145–150	191.45	0.09	0.08	0.031	0.034	1,753	1,714	1,294	1,254	3.99	3.63	12.6	15.6	1.85	1.02
25X-2, 140–145	215.90	0.14	0.13	0.030	0.036	2,368	2,292	1,395	1,343	5.64	5.53	16.2	13.0	1.42	1.48

Table T3 (continued).

Core, section, interval (cm)	Depth (mbsf)	Trace elements (ppm)			
		V		Zr	
		Flux	Microwave	Flux	Microwave
206-1256B-					
1H-1, 145–150	1.45	122.5	153.5	139.9	157.1
1H-2, 70–75	2.20	120.1	107.8	151.4	145.3
1H-4, 70–75	5.20	100.0	96.7	125.5	121.8
2H-1, 142–147	7.52	75.1	69.1	107.2	104.8
2H-2, 0–75	8.27	106.1	99.8	148.7	149.6
2H-2, 145–150	9.02	86.6	86.7	149.4	157.8
3H-3, 145–150	20.05	67.1	58.9	172.3	162.3
3H-4, 70–75	20.80	195.0	182.4	159.7	163.2
3H-5, 70–75	22.30	98.5	102.1	151.8	157.6
3H-5, 145–150	23.05	110.4	115.1	162.7	158.3
4H-1, 145–150	26.55	160.9	155.5	151.0	144.1
4H-2, 145–150	28.05	80.8	80.1	129.9	126.0
4H-5, 145–150	32.55	89.0	88.8	115.1	126.2
4H-7, 71–76	34.81	77.2	74.6	128.7	134.5
5H-2, 145–150	37.55	62.9	70.5	121.9	123.9
5H-4, 145–150	40.55	64.5	74.3	118.1	116.2
5H-6, 145–150	43.55	140.4	134.4	111.5	100.9
6H-5, 145–150	51.55	82.6	83.4	106.8	105.6
6H-7, 65–70	53.75	217.2	225.0	100.0	112.5
7H-5, 145–150	61.05	27.9	20.7	57.7	59.3
8H-2, 145–150	66.05	64.5	53.3	59.2	62.7
8H-5, 145–150	70.55	10.9	9.0	43.9	45.2
10H-2, 145–150	85.05	41.2	32.6	103.4	93.6
10H-5, 145–150	89.55	26.5	28.8	101.6	92.6
11H-2, 145–150	94.55	18.2	16.0	88.0	96.0
12H-5, 145–150	108.55	36.3	28.2	32.6	34.2
14H-5, 145–150	127.55	7.0	5.1	8.6	10.2
15H-5, 145–150	137.05	1.5	1.3	10.0	10.7
16H-2, 145–150	142.05	1.9	1.6	10.6	11.2
17H-5, 145–150	156.05	8.4	6.0	11.5	9.0
18H-1, 95–100	159.05	21.9	17.2	7.6	8.3
20X-2, 145–150	168.15	19.1	15.4	14.8	14.6
20X-5, 145–150	172.65	14.8	16.4	9.6	7.7
22X-5, 145–150	191.45	13.6	9.8	10.6	8.4
25X-2, 140–145	215.90	19.2	16.4	9.8	10.0

Table T4. Descriptive statistics of shore-based flux fusion vs. shore-based microwave-assisted acid digestion comparison.

Element	Correlation coefficient	Slope	y-intercept
Si	0.982	0.936	0.56
Al	0.999	0.976	0.01
Ti	0.998	1.002	0.00
Fe	0.997	0.949	0.07
Mn	0.998	0.990	–0.01
Ca	0.994	0.997	–0.03
Mg	0.995	0.993	–0.02
Na	0.989	0.945	0.04
K	0.997	0.992	0.01
P	0.961	0.943	0.01
Ba	0.995	1.006	5.31
Sr	0.995	1.017	–39.72
Cr	0.981	0.884	–0.09
Ni	0.971	0.842	32.21
Sc	0.996	1.009	–0.05
V	0.991	1.014	–2.44
Zr	0.994	0.998	0.43

Table T5. Results from Boston University microwave acid digestions at a higher sampling resolution. (**See table notes.** Continued on next two pages.)

Core, section, interval (cm)	Depth (mbsf)	Age (Ma)	Major elements (wt%)										Trace elements (ppm)						
			Si	Al	Ti	Fe	Mn	Ca	Mg	Na	K	P	Ba	Sr	Cr	Ni	Sc	V	Zr
206-1256B-																			
1H-1, 70–75	0.70	0.060	22.40	5.50	0.256	3.84	1.315	6.59	1.15	2.25	1.70	0.120	6,058	520	28.46	293	16.15	119.6	131.2
1H-1, 145–150	1.45	0.124	25.25	7.17	0.400	5.87	0.555	1.25	1.58	1.61	1.31	0.161	8,419	437	71.78	389	23.07	153.5	157.1
1H-2, 70–75	2.20	0.188	19.50	5.05	0.271	4.44	0.696	3.45	1.59	2.79	1.20	0.132	7,949	445	42.30	816	19.48	107.8	145.3
1H-2, 145–150	2.95	0.253	22.59	5.57	0.316	5.10	0.866	4.53	1.81	3.08	1.18	0.144	8,375	514	42.78	614	21.28	86.3	150.8
1H-3, 70–75	3.70	0.317	26.30	6.14	0.263	3.27	0.966	1.97	1.17	2.80	2.20	0.084	6,242	354	30.96	483	14.64	71.0	147.3
1H-470–75	5.20	0.445	19.79	5.03	0.280	3.93	0.700	7.95	1.50	2.00	1.17	0.132	6,267	565	42.60	682	18.45	96.7	121.8
1H-4, 122–127	5.72	0.490	21.80	5.26	0.305	4.33	0.420	5.87	1.85	4.03	1.38	0.110	7,771	538	37.17	754	18.87	137.8	143.0
2H-1, 73–78	6.83	0.585	16.55	4.62	0.252	3.31	0.448	17.28	1.37	1.69	1.04	0.148	9,930	873	43.63	738	16.28	72.9	100.2
2H-1, 142–147	7.52	0.644	16.09	4.60	0.239	3.20	0.405	12.46	1.30	1.56	1.12	0.142	10,155	828	46.23	562	16.37	69.1	104.8
2H-2, 0–75	8.27	0.708	22.36	6.07	0.349	5.22	0.325	2.03	1.82	3.04	1.30	0.183	9,209	420	47.15	465	22.28	99.8	149.6
2H-2, 145–150	9.02	0.772	22.32	5.92	0.331	4.86	0.500	4.13	1.57	1.51	1.20	0.158	8,992	492	47.45	484	22.23	86.7	157.8
2H-3, 70–75	9.77	0.837	23.80	6.15	0.357	5.12	0.660	3.88	1.95	3.37	1.38	0.155	10,138	534	49.46	703	23.72	82.8	152.4
2H-3, 145–150	10.52	0.901	20.46	5.01	0.279	4.01	0.697	9.23	1.40	1.67	1.17	0.148	8,915	654	38.34	625	18.16	70.7	151.1
2H-4, 70–75	11.27	0.965*	23.78	5.69	0.326	3.89	0.355	4.74	1.62	3.53	1.95	0.12	7,711	500	30.31	718	16.30	142.2	262.3
2H-4, 145–150	12.02	1.029*	19.38	5.00	0.260	3.67	2.608	7.98	1.64	2.23	1.43	0.14	7,760	544	39.42	588	17.77	111.6	131.6
2H-5, 70–75	12.77	1.093	15.43	4.49	0.247	3.54	0.902	12.11	1.41	2.27	1.05	0.143	7,109	682	39.18	479	16.54	74.1	125.2
2H-5, 145–150	13.52	1.158	19.61	5.55	0.305	4.41	0.734	7.60	1.67	2.23	1.23	0.159	9,158	604	43.80	635	19.64	84.7	140.6
2H-6, 70–75	14.27	1.242	19.86	5.42	0.304	4.19	0.324	7.93	1.75	2.63	1.42	0.128	8,341	595	45.41	750	21.10	196.8	151.0
2H-6, 145–150	15.02	1.361	17.03	4.25	0.214	2.91	5.729	7.15	2.04	2.09	1.18	0.111	6,444	355	34.52	698	13.73	395.8	108.9
2H-7, 63–68	15.70	1.469	21.12	5.31	0.278	4.54	0.431	10.36	1.56	2.04	1.29	0.138	7,734	599	36.68	543	17.87	99.6	144.0
3H-1, 70–75	16.30	1.565	20.64	5.80	0.315	5.03	1.117	5.59	1.68	1.52	1.26	0.156	10,803	570	48.87	498	22.32	91.0	158.0
3H-1, 145–150	17.05	1.684	5.09	1.17	0.058	0.98	6.211	13.10	2.08	0.58	0.32	0.076	1,458	205	10.57	114	3.84	29.8	33.4
3H-2, 70–75	17.80	1.803	24.84	6.18	0.319	5.91	0.757	1.98	1.94	3.48	1.80	0.133	11,026	447	34.12	424	18.91	94.7	183.4
3H-2, 145–150	18.55	1.922	24.27	6.37	0.344	6.00	0.366	1.53	1.93	2.78	1.55	0.160	11,705	435	54.82	497	21.46	93.4	188.1
3H-3, 70–75	19.30	2.041	23.49	6.71	0.365	6.00	1.814	1.55	1.97	2.56	1.69	0.220	12,963	507	38.11	419	21.35	98.6	175.2
3H-3, 145–150	20.05	2.160	23.47	5.90	0.243	3.36	1.929	1.56	1.20	2.10	2.20	0.143	8,467	357	32.57	576	13.28	58.9	162.3
3H-4, 70–75	20.80	2.280	22.13	5.95	0.322	4.82	0.309	5.00	1.80	2.55	1.46	0.154	13,554	633	52.14	614	21.19	182.4	163.2
3H-4, 145–150	21.55	2.399	23.57	6.32	0.354	4.90	0.363	3.34	1.97	2.67	1.52	0.165	14,226	544	50.89	641	22.55	163.4	162.6
3H-5, 70–75	22.30	2.518	23.59	6.67	0.360	4.77	0.204	1.20	1.89	2.58	1.59	0.153	13,524	469	53.63	637	22.95	102.1	157.6
3H-5, 145–150	23.05	2.637	24.94	6.65	0.358	4.70	0.201	1.18	1.86	2.46	1.58	0.170	13,780	482	58.05	726	21.81	115.1	158.3
3H-6, 145–150	24.55	2.875	24.54	6.57	0.366	4.73	0.528	1.55	1.84	2.63	1.54	0.260	15,688	479	70.05	698	25.90	88.7	172.7
3H-7, 57–62	25.17	2.974	22.55	6.10	0.333	4.26	0.600	4.45	1.54	2.45	1.45	0.197	13,267	583	62.00	451	22.25	76.0	153.9
4H-1, 145–150	26.55	3.193	22.37	6.53	0.359	4.63	0.506	2.62	2.11	2.66	1.43	0.182	13,643	508	69.67	630	22.63	155.5	144.1
4H-2, 145–150	28.05	3.431	19.66	5.37	0.296	3.76	0.481	5.90	1.65	2.46	1.19	0.139	11,851	575	60.40	579	19.92	80.1	126.0
4H-3, 145–150	29.55	3.670	22.07	6.07	0.329	4.46	0.516	5.23	1.84	2.59	1.44	0.179	10,464	531	62.28	510	23.18	81.2	143.3
4H-4, 145–150	31.05	3.908	23.47	6.31	0.367	4.58	3.276	1.19	2.10	2.14	1.18	0.216	12,308	507	47.22	1,067	23.49	127.1	138.2
4H-5, 145–150	32.55	4.146	19.26	5.63	0.296	3.79	2.697	4.84	1.92	2.50	1.18	0.243	11,100	520	62.05	941	20.84	88.8	126.2
4H-6, 145–150	34.05	4.385	27.69	6.62	0.305	3.76	0.790	2.52	1.66	2.68	1.81	0.141	10,218	470	52.45	442	18.90	80.7	125.2
4H-7, 71–76	34.81	4.506	20.13	5.69	0.296	3.89	1.176	6.70	1.67	2.00	1.15	0.165	13,048	725	52.87	690	22.18	74.6	134.5
5H-1, 145–150	36.05	4.703	19.35	4.88	0.261	3.36	1.327	12.13	1.48	2.01	1.08	0.154	15,302	857	38.87	699	17.38	60.5	117.3
5H-2, 145–150	37.55	4.941	20.62	5.36	0.256	3.29	0.809	9.27	1.44	2.30	1.35	0.141	14,591	787	41.18	677	18.01	70.5	123.9
5H-3, 145–150	39.05	5.179*	13.87	3.66	0.182	2.42	0.834	22.13	1.05	1.50	0.75	0.12	12,230	1,154	36.09	482	12.74	44.0	79.3
5H-4, 145–150	40.55	5.340	21.54	4.42	0.227	3.41	0.549	7.37	1.46	1.98	1.08	0.136	19,369	782	46.36	665	18.29	74.3	116.2
5H-5, 145–150	42.05	5.451	18.51	4.14	0.215	2.88	0.475	20.71	1.37	2.50	0.96	0.150	13,191	921	59.20	666	14.69	105.1	85.6
5H-6, 145–150	43.55	5.561	21.02	4.17	0.221	3.23	0.352	13.27	1.62	2.53	1.06	0.145	15,598	863	35.95	632	16.88	134.4	100.9
5H-7, 66–71	44.26	5.614*	22.82	4.74	0.262	3.46	0.369	8.74	1.75	2.64	1.25	0.15	15,680	804	47.84	702	18.82	103.9	126.3

Table T5 (continued).

Core, section, interval (cm)	Depth (mbsf)	Age (Ma)	Major elements (wt%)										Trace elements (ppm)						
			Si	Al	Ti	Fe	Mn	Ca	Mg	Na	K	P	Ba	Sr	Cr	Ni	Sc	V	Zr
6H-1, 145–150	45.55	5.709	24.64	4.43	0.233	3.19	1.104	4.22	1.78	2.46	1.20	0.160	15,540	645	37.68	891	18.41	72.7	111.0
6H-2, 145–150	47.02	5.817*	19.80	3.12	0.162	2.44	0.509	15.80	1.30	1.58	0.99	0.12	12,969	958	29.54	505	13.60	72.6	101.7
6H-3, 145–150	48.55	5.930	12.96	2.51	0.132	1.80	0.444	22.70	0.83	1.02	0.62	0.111	7,971	1,276	28.93	487	9.88	31.6	68.0
6H-4, 145–150	50.05	6.040	13.33	3.07	0.154	1.84	0.436	21.23	1.01	1.59	0.74	0.113	7,434	1,307	27.62	524	10.38	47.0	65.1
6H-5, 145–150	51.55	6.151	23.88	4.27	0.217	2.84	0.309	5.73	1.56	2.19	1.08	0.194	12,782	685	31.95	863	16.97	83.4	105.6
6H-6, 145–150	53.05	6.261	24.21	4.21	0.226	3.49	0.371	5.28	2.08	2.20	1.04	0.189	12,271	611	32.23	1,063	17.43	209.1	115.5
6H-7, 65–70	53.75	6.313	23.81	4.35	0.224	2.89	0.355	4.64	1.66	1.97	1.12	0.183	11,790	580	37.98	1,106	18.02	225.0	112.5
7H-1, 145–150	55.05	6.409	21.25	3.06	0.151	2.04	0.382	11.81	1.24	1.91	0.94	0.166	11,668	953	21.69	526	12.70	51.4	86.3
7H-2, 145–150	56.55	6.519	22.10	3.50	0.167	2.20	1.330	6.33	1.38	2.24	0.98	0.161	11,615	698	23.16	447	13.23	48.0	89.5
7H-5, 145–150	61.05	6.850	15.36	2.09	0.109	1.47	0.405	18.80	0.85	1.30	0.61	0.111	11,204	1,261	17.16	479	8.50	20.7	59.3
8H-2, 145–150	66.05	7.219	24.72	2.00	0.090	1.33	0.264	9.82	0.95	2.00	0.70	0.057	9,953	670	15.28	532	7.73	53.3	62.7
8H-5, 145–150	70.55	7.550	11.74	1.32	0.071	1.12	1.311	23.14	0.76	1.24	0.43	0.079	8,687	1,309	9.83	537	5.72	9.0	45.2
9H-2, 145–150	75.55	7.967	11.40	1.26	0.062	1.35	0.563	25.83	0.67	1.33	0.45	0.064	6,968	1,428	10.17	226	5.59	15.5	49.4
10H-2, 145–150	85.05	9.080	23.29	2.18	0.115	2.26	0.800	12.36	1.03	1.53	0.73	0.110	11,156	844	15.18	240	10.26	32.6	93.6
10H-5, 145–150	89.55	9.607*	33.34	2.03	0.120	2.05	0.111	0.50	0.98	1.96	0.63	0.044	10,211	328	15.70	179	9.95	28.8	92.6
11H-2, 145–150	94.55	10.193	22.31	1.13	0.070	1.21	0.159	13.68	0.64	1.41	0.41	0.069	8,821	914	16.00	101	7.56	16.0	96.0
11H-5, 145–150	99.05	10.446	12.69	1.85	0.092	0.64	0.161	28.59	0.44	1.56	0.26	0.046	4,641	1,325	5.70	48	4.34	5.9	30.7
12H-2, 145–150	104.05	10.583	17.07	2.42	0.107	2.91	0.152	15.95	1.25	2.40	1.00	0.105	12,637	1,134	18.57	70	11.55	23.6	87.9
12H-5, 145–150	108.55	10.706	13.55	1.11	0.048	0.96	0.187	25.53	0.53	1.06	0.28	0.050	6,888	1,350	8.27	75	4.60	28.2	34.2
13H-2, 145–150	112.85	10.824	35.50	0.25	0.018	0.27	0.057	6.28	0.38	1.80	0.10	0.010	1,795	400	3.39	15	1.70	31.0	15.2
13H-5, 95–100	116.85	10.934	14.22	0.63	0.031	0.94	0.209	28.00	0.51	1.11	0.32	0.054	4,994	1,318	2.86	36	5.51	6.4	31.2
14H-2, 145–150	123.05	11.104	5.27	0.29	0.018	0.49	0.222	36.26	0.28	0.77	0.15	0.049	2,255	1,725	2.59	37	2.51	7.2	15.2
14H-5, 145–150	127.55	11.228	4.99	0.15	0.009	0.22	0.187	33.89	0.19	0.55	0.07	0.037	1,349	1,749	0.99	26	1.28	5.1	10.2
15H-2, 145–150	132.55	11.365	6.20	0.12	0.007	0.33	0.160	31.21	0.22	0.51	0.17	0.029	1,911	1,513	3.73	11	1.89	2.1	16.2
15H-5, 145–150	137.05	11.489	11.98	0.12	0.006	0.30	0.130	30.31	0.26	0.78	0.09	0.026	2,208	1,301	0.99	29	1.30	1.3	10.7
16H-2, 145–150	142.05	11.626	7.71	0.21	0.010	0.36	0.141	30.15	0.29	0.55	0.11	0.032	2,316	1,338	3.13	24	1.90	1.6	11.2
16H-5, 145–150	146.55	11.749	4.92	0.20	0.011	0.45	0.159	32.01	0.23	0.65	0.09	0.034	1,973	1,355	0.81	35	1.25	2.6	11.7
17H-2, 145–150	151.60	11.888	12.01	0.14	0.007	0.23	0.129	26.79	0.31	1.05	0.11	0.032	2,269	1,152	3.36	12	1.51	5.7	9.6
17H-5, 145–150	156.05	12.010*	8.52	0.14	0.007	0.41	0.117	30.38	0.32	0.77	0.09	0.044	2,090	1,274	3.57	16	1.43	6.0	9.0
18H-1, 95–100	159.05	12.093	7.44	0.13	0.005	0.28	0.100	31.72	0.31	0.69	0.08	0.038	1,986	1,184	1.41	9	1.18	17.2	8.3
19X-1, 145–150	161.60	12.162	9.39	0.23	0.007	0.35	0.086	31.08	0.30	1.30	0.09	0.039	2,395	1,209	1.80	28	1.82	15.1	14.7
19X-2, 145–150	163.05	12.202	7.94	0.19	0.005	0.38	0.077	31.88	0.25	0.71	0.09	0.037	2,186	1,252	2.38	17	1.45	11.5	12.0
20X-2, 145–150	168.15	12.342	2.95	0.10	0.004	0.37	0.085	33.93	0.24	0.45	0.06	0.039	1,335	1,165	4.24	21	0.93	15.4	14.6
20X-5, 145–150	172.65	12.466	3.90	0.15	0.006	0.33	0.097	33.77	0.19	0.47	0.06	0.036	1,638	1,228	4.73	24	1.12	16.4	7.7
21X-2, 145–150	177.75	12.606	5.07	0.25	0.012	0.61	0.104	31.47	0.29	0.63	0.13	0.038	2,767	1,399	4.53	29	1.69	16.1	16.7
21X-4, 145–150	180.75	12.688	7.51	0.14	0.007	0.50	0.133	31.53	0.25	0.65	0.08	0.036	1,960	1,342	2.94	24	1.03	16.6	8.5
22X-2, 140–145	186.90	12.857	9.05	0.11	0.005	0.67	0.103	31.66	0.21	0.51	0.07	0.036	1,763	1,130	3.37	24	0.72	11.7	7.6
22X-5, 145–150	191.45	12.982	5.90	0.12	0.007	0.28	0.140	31.71	0.22	0.82	0.08	0.034	1,714	1,254	3.63	16	1.02	9.8	8.4
23X-2, 140–145	196.60	13.123	4.36	0.18	0.007	0.72	0.165	30.91	0.29	0.91	0.10	0.036	2,347	1,297	3.57	35	1.30	6.9	8.5
23X5, 145–150	201.15	13.248	7.10	0.20	0.011	0.47	0.119	30.49	0.31	0.93	0.11	0.042	2,512	1,293	6.40	20	1.56	6.9	9.9
24X-2, 140–145	206.30	13.389	3.56	0.19	0.007	0.44	0.146	32.91	0.31	0.80	0.10	0.042	2,711	1,405	3.13	17	1.25	6.9	9.0
24X-4, 145–150	209.40	13.475*	1.29	0.18	0.007	0.57	0.150	34.96	0.33	0.67	0.15	0.045	2,711	1,518	3.33	15	1.20	17.4	9.1
25X-2, 140–145	215.90	13.653	1.24	0.13	0.006	0.51	0.217	37.48	0.32	0.64	0.13	0.036	2,292	1,343	5.53	13	1.48	16.4	10.0
25X-2, 145–150	215.95	13.654	1.29	0.12	0.005	0.46	0.228	37.68	0.29	0.43	0.13	0.031	2,259	1,332	5.62	13	1.34	16.3	9.9
26X-1, 105–115	223.75	13.868	4.77	0.33	0.014	2.29	0.250	33.89	0.96	0.43	0.40	0.058	3,778	1,257	7.39	42	2.89	11.9	28.3
26X-3, 30–40	226.00	13.930	4.34	0.35	0.014	1.72	0.242	35.47	1.25	0.51	0.31	0.045	2,135	1,132	8.92	41	2.68	10.7	27.7
27X-CCW	226.00		3.42	0.16	0.006	0.96	0.375	34.64	0.42	0.79	0.30	0.045	2,407	1,080	7.41	30	1.43	8.9	12.5

Table T5 (continued).

Core, section, interval (cm)	Depth (mbsf)	Age (Ma)	Major elements (wt%)										Trace elements (ppm)						
			Si	Al	Ti	Fe	Mn	Ca	Mg	Na	K	P	Ba	Sr	Cr	Ni	Sc	V	Zr
206-1256C-																			
3R-1, 140–150	240.40	14.325	1.05	0.15	0.005	0.62	0.373	37.60	0.28	0.42	0.29	0.031	1,645	1,332	6.54	17	1.22	9.1	8.2
3R-2, 140–145	241.90	14.367	0.95	0.13	0.005	0.59	0.368	37.47	0.29	0.48	0.29	0.031	2,011	1,188	6.32	16	1.09	15.6	10.5
3R-3, 131–141	243.30	14.405	1.62	0.13	0.004	0.74	0.357	36.17	0.35	0.59	0.38	0.041	2,112	1,144	7.71	12	1.19	33.6	11.4
4R-1, 0–5	245.00	14.452	5.43	0.27	0.012	2.82	0.265	33.38	0.85	0.30	1.53	0.047	2,934	1,274	9.71	15	1.88	28.0	20.0

Notes: * = average of three replicate. Data overspecified for calculation purposes. See text for discussion of true analytical precision.

Table T6. Descriptive statistics of shipboard flux fusion vs. shore-based microwave-assisted acid digestion comparison.

Element	Correlation coefficient	Slope	y-intercept
Si	0.986	0.861	–1.51
Al	0.995	0.863	–0.06
Ti	0.991	0.792	0.00
Fe	0.987	0.859	–0.145
Mn	0.694	0.654	0.08
Ca	0.992	0.976	2.26
Mg	0.978	0.852	–0.04
Na	0.963	0.668	0.56
K	0.987	0.798	0.11
Ba	0.970	0.889	73.44
Sr	0.953	1.391	94.81
Cr	0.037	0.029	16.29
V	0.964	0.808	0.71
Al/Ti	0.543	0.335	13.15
Ba/Ti	0.871	1.036	10,599
Fe/Al	0.910	0.864	1.71